University of Pennsylvania
ScholarlyCommons

Departmental Papers (MEAM)

Department of Mechanical Engineering & Applied Mechanics

Dynamic Rolling for a Modular Loop Robot

Jimmy Sastra
University of Pennsylvania

Sachin Chitta
University of Pennsylvania

Mark Yim
University of Pennsylvania, yim@seas.upenn.edu

Follow this and additional works at: http://repository.upenn.edu/meam_papers

Part of the Applied Mechanics Commons

Dynamic Rolling for a Modular Loop Robot

Abstract

Reconfigurable modular robots use different gaits and configurations to perform various tasks. A rolling gait is the fastest currently implemented gait available to a modular robot for traversal of level ground. In this work, we analyze and implement a sensor-based feedback controller to achieve dynamic rolling for a 10 module loop robot. The controller exploits the dynamics of the system to build up momentum in each step by specifying a desired global shape for the robot at touchdown. Energy is input into the system both by raising the height of the center of mass of the robot and moving the position of center of mass with respect to the ground to maximize the moment arm due to gravity. Using simulation and experimental results, we show how the desired shape can be varied to achieve higher terminal velocities. Through simulation, we also show rounder shapes have lower specific resistance and are thus more efficient.

Keywords

dynamic, rolling, modular, robot

Disciplines

Applied Mechanics | Engineering | Mechanical Engineering

Comments

Dynamic Rolling for a Modular Loop Robot

Jimmy Sastra, Sachin Chitta, and Mark Yim

GRASP Lab, University of Pennsylvania, Philadelphia, PA, USA
{jsastra,sachinc,yim}@grasp.upenn.edu

Summary. Reconfigurable modular robots use different gaits and configurations to perform various tasks. A rolling gait is the fastest currently implemented gait available to a modular robot for traversal of level ground. In this work, we analyze and implement a sensor-based feedback controller to achieve dynamic rolling for a 10 module loop robot. The controller exploits the dynamics of the system to build up momentum in each step by specifying a desired global shape for the robot at touchdown. Energy is input into the system both by raising the height of the center of mass of the robot and moving the position of center of mass with respect to the ground to maximize the moment arm due to gravity. Using simulation and experimental results, we show how the desired shape can be varied to achieve higher terminal velocities. Through simulation, we also show rounder shapes have lower specific resistance and are thus more efficient.

1 Introduction

Reconfigurable modular robots can locomote using different gaits in a variety of configurations [1, 2, 5, 10]. The choice of configuration is usually task specific. Certain configurations are more suitable for locomotion in constrained spaces (e.g. snake like) while others may be more useful over rough terrain (walking robot configurations). On flat terrain, the closed loop configuration shown in Figure 1(a) is currently considered to be the most efficient as well as the fastest configuration under some conditions [10] (this has not been proven for the general case though). It has been implemented on various robots in [5, 9, 10]. In all of these implementations, the gaits implemented were *kinematic*, *ie* there was no inertial component to the motion, setting the inputs of the robot to zero would stop the robot. There is a limit to the rate at which a kinematic rolling track can accelerate. Accelerating too fast causes the loop to undulate in place or worse roll backwards as shown in Figure 1(c). In [4], Kamimura et al implemented an *open-loop* dynamic rolling gait using CPGs where the weights for the CPGs were determined using simulation. In [7], Matsuda and Murata proposed a closed-link robot where the actuators control the stiffness of a spring in each joints. This allows them to adjust the *stiffness* in each joint and drive the robot forward. In [8], a dynamic simulator was used to generate and simulate a

dynamic rolling gait. Feedback was through accelerometers in the robot and an average velocity of about 1 m/s was reported. However, this gait was not implemented on an actual robot and no analytical insight was provided.

In this work, we present a new implementation of the rolling loop using sensor-based feedback. Our work differs from previous work in the use of sensory feedback, development of a simplified dynamic model that provides considerable insight for development of control and implementation on a prototype robot. Sensory feedback dramatically improves the reliability of this gait (as compared to open loop implementations). The rolling loop is a closed loop system and thus hard to simulate. A complete 10 degree of freedom model could be built for our robot but it results in complex equations and may not provide much insight into the dynamics of the system. Further, with 10 actuators on the robot, the input space is big and designing controllers for such a robot is non-trivial. Our approach is to simplify the model for the system by restricting the type of controller to track an appropriate shape at *touchdown*, the contact of a module with the ground. In addition the method scales to any number of modules or joints in a loop. By our choice of controller, we are able to control the shape of the robot by varying a single parameter. In addition to simplifying the control algorithm, our approach also offers better insight into the dynamics of the system.

This paper is structured as follows. In Section 2, we present the robot used in this work. In Section 3, we propose the framework used for control. In Section 4 we present a simple four-bar like model for the robot. In Section 5, we present theoretical results derived using this model. Experimental results are also presented in Section 5. In Section 6, we follow up with a discussion on insight gained from the results and possible future applications.
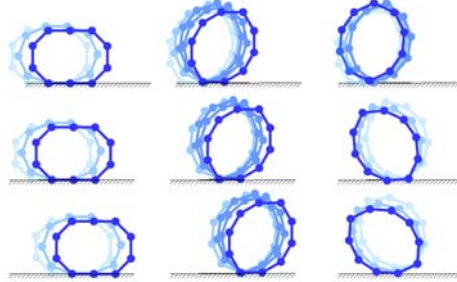

Fig. 1. (a) Kinematic Rolling (b) Dynamic Rolling: Ideal Case (c) Dynamic Rolling: Loop turns back on itself.

2 The robot

The modular robot used in this work is shown in Figure 2(a). An individual module is shown in Figure 2(b). Each module is made up of a hobby servo that drives a rotary degree of freedom. Communication is through a global bus based on the RoboticsBus protocol [3] which is built on the CANbus standard (Controller Area Network). Control signals are provided to individual modules at 60 Hz. A separate add-on microcontroller board serves as a controller. It plugs into one of the ports on the robot (there are seven external and one internal ports) and provides control signals for all modules. Control is implemented by specifying a desired angular position for each servo at 60 Hz. This translates into a desired shape of the robot. Touchdown is detected using custom-built sensors plugged into a port on the inside of each module. The sensors used here are IR based proximity sensors that indicate distance to the ground. This information is put on the bus at 60 Hz. The controller determines touchdown using pre-determined thresholds for the sensors on different surfaces.
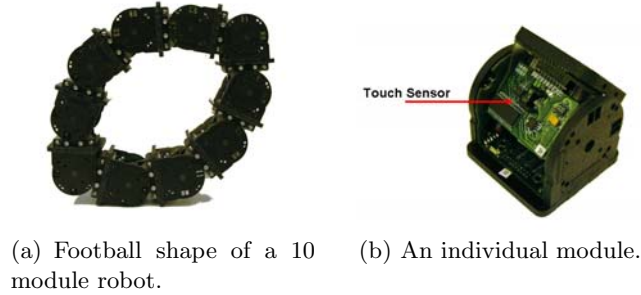

(a) Football shape of a 10 module robot.   (b) An individual module.

Fig. 2. The modular robot used for experiments.

3 Control

3.1 Kinematic Rolling

A kinematic roll is often implemented by repeatedly moving the shape of the loop such that the long axis rotates. One rotation of the long axis would be one cycle of the gait. The frequency of rotation is directly proportional to the speed, *ie* stopping the tread causes the whole robot to stop. For a closed loop robot like the one used in this work, one typical loop shape has two lines of modules one on top of the other attached by an intermediate set of modules as shown in Figure 1(a). A kinematic roll is now executed by smoothly interpolating the position of each module to the next one in the loop. This type of motion can be easily represented using a *gait table* [10].

3.2 Dynamic Rolling

To create a dynamic rolling motion, the basic approach is to move the center of mass beyond the pivot point for the module currently on the ground (Figure 1(b)

and Figure 4). This results in a moment contribution from the weight of the robot in the direction of rolling and the robot accelerates in that direction. The motion of the robot after touchdown can be separated into two phases: (1) a shape change where the robot changes shape to the new desired shape that increases the distance between the center of mass and the ground contact point and (2) a falling phase where the robot's shape is frozen and the robot behaves essentially like an inverted pendulum pivoting about the contact point. In this paper, we will show that the first phase results in a slight deceleration while in the second phase the robot is continuously accelerating towards the next touchdown. We restrict the shape of the
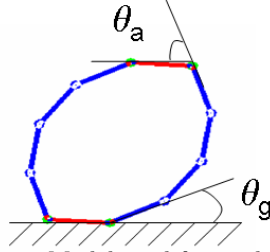

Fig. 3. Model used for analysis.

robot to a shape as shown in Figure 3 that is formed by joining two equal arcs of a circle. In the limit, as the two arcs approach a semi-circle, the shape reduces to a circle. The modules of the robot approximate these arcs of a circle to form the desired shape in Figure 3 which closely resembles an American football shape. The shape can be defined using a single parameter- θ_a, the angle between the modules at the top and bottom apex of the shape (Figure 3). All the other joint angles are equal to each other (to say θ_s) and can be derived in terms of θ_a using the expression $2\theta_a + 8\theta_s = 2\pi$. Note that although the robot shown uses 10 modules, these two joint angles are all that are required for any number of modules. More elongated shapes (corresponding to higher values of θ_a) will result in a bigger moment arm and higher angular acceleration. However, the amount of shape change (represented by the net change of joint angles) is also much higher. Rounder shapes correspond to a smaller value of θ_a and will result in a smaller moment arm and smaller amount of shape change. Thus, we should expect that more elongated shapes will give us higher accelerations while rounder shapes may be more efficient. We will examine the effect of the desired shape on the speed of the robot by varying the single parameter (θ_a).

An important point to note for this controller is that during a shape change, the joint angles for only four modules will be transitioning while the joint angles for all other modules remain fixed. We will exploit this crucial property, a consequence of choosing this particular controller, in developing a simplified model for dynamic rolling in the next section.

In addition to the change of shape, another parameter that plays an important role in the gait is the speed at which this shape change is carried out. To get initial acceleration, we need to start out with a finite rate of change of shape. Choosing too high an initial rate change will cause the robot to accelerate suddenly and may result in undesirable dynamic modes where the robot falls backwards (Figure 1(c)). Too low a rate may not be sufficient to get the robot started. Further, as the robot

moves faster, the shape change rate needs to be adjusted so that shape change occurs before the next touchdown happens. At higher rolling speeds of the robot, it is also beneficial to reduce the amount of shape change, *ie* make the desired shape *rounder*. Thus, we now have a discrete control algorithm applied at every touchdown that specifies two parameters: (1) the new desired shape by specifying θ_a and (2) the shape change rate to converge to the desired shape.

4 Analytical model

To simplify the modeling of dynamic rolling we first observe that only four modules are moving at a time. We can thus simplify the model of the loop to that of a floating four-bar mechanism. The two longer arcs (nodes 2 through 5 and nodes 7 through 10) represent two of the links of the four-bar while the other two links (comprising node 1 and 6) are made up of single modules. This framework is shown in Figure 4.
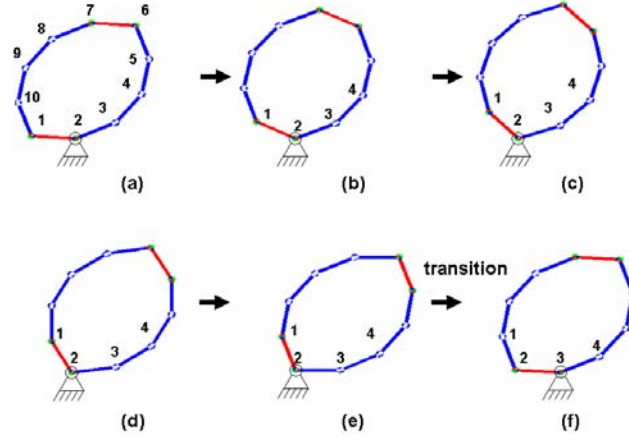

Fig. 4. Phases of dynamic rolling.

We define a *step* of the gait as the sequence of events between consecutive touchdowns of two adjacent modules. At touchdown, θ_a is decreased to θ_s. This part of the step is illustrated in Figure 4(b). Once it reaches the new desired position, the local shape does not deform anymore. Now, the robot undergoes a pure falling motion (Figure 4(d)). The robot falls like an inverted pendulum until node 3 touches down on the ground (Figure 4(e)). At this point, we reassign the nodes to the different links based on the global positions of the nodes. Thus, now node 2 forms one link for the four bar as does node 7. Nodes 3 through 6 and nodes 8 through 1 comprise the other 2 links of the four-bar (Figure 4(f)). Reducing the model in this manner manner to the one degree of freedom four bar linkage implies that the shape of the robot can be parameterized using a single parameter, the angle at the apex θ_a (or similarly θ_s).

The equations of motion for this simplified version of the robot are derived using a standard method by first defining the Lagrangian for the system and deriving Lagrange's equations. The generalized coordinates used in the analysis are the apex angle θ_a and the global angle made by the robot with the ground θ_g (Figure 3). The mass of the modules is assumed to be 0.138kg. Each module is considered to be a thin rod of length 0.06 m. The resultant equation for the evolution of θ_g can be expressed in the form:

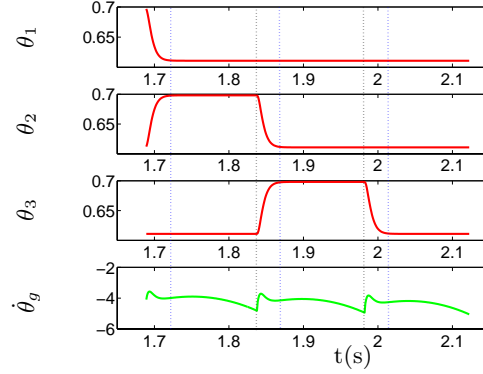$$\ddot{\theta}_g = f_1(\theta_a, \theta_g)mg + f_2(\tau). \tag{1}$$

Fig. 5. (a) Joint angle for Module 1 (b) Joint angle for Module 2 (c) Joint angle for Module 3 (d) Angular velocity of the robot over time interval corresponding to three consecutive module touchdowns.

Equation 1 shows that there are two contributing terms to the angular acceleration of the robot: (1) the moment due to gravity about the point of contact with the ground and (2) a coupling term arising from the coupling of θ_a and θ_g. The shape change phase causes decceleration of the robot while the moment due to gravity constantly contributes in the direction of roll of the robot. Thus, as soon as the robot is done changing shape, it accelerates. This can be seen from the plot of angular velocity in Figure 5. As Module 1 touches down and the controller starts changing the shape of the robot, the robot initially decelerates. The robot starts accelerating solely under the influence of gravity in the direction of rolling as soon as the shape change phase finishes.

When the module comes into contact with the ground, a transition condition is defined at impact of the module on the ground. Joint angles and the position of the robot stay fixed at transition while velocities are transformed using the transition conditions. The transition condition relates the angular momentum L_- of the whole body of the robot about the new pivot point on the ground just before impact with the angular momentum L_+ of the whole body about the new pivot point after impact. Using a coefficient of restitution η (found empirically to be 0.94),

the transition condition is given by the following momentum transfer equation on impact: $L_+ = \eta L_-$.

5 Results

5.1 Theoretical results

Multiple simulations were run with different desired shapes for the robot at touchdown. We are primarily interested in two quantities in simulation: (1) The terminal velocities we can achieve with different shapes and (2) a measure of the energy efficiency of the robot. Energy efficiency is measured using a quantity called *specific resistance* which is calculated as

$$\epsilon = \frac{P}{mgv} \tag{2}$$

where P is the power input to the robot, g is the acceleration due to gravity and v is the average speed of the robot. Power is calculated for the theoretical model as $P = \tau\dot{\theta}$. This power is only a part of the net power input to the robot and only takes into account the power required to effect shape change in the robot.

Figure 8 plots the final speed of the robot for different desired shapes at touchdown. As the desired shape becomes more and more elongated, the final terminal speed achieved by the robot increases. The terminal speed can be explained by the loss of energy at impact. Eventually, the controller is putting in just enough energy to overcome that loss. As the desired shape grows elongated (θ_a increases), the angular acceleration of the robot in its free fall phase also increases thus resulting in a higher terminal speed.

Figure 6 plots the specific resistance for different desired shapes. While the power measured here in calculating specific resistance is lower than the actual power input to the robot, we believe the trend will stay the same, *ie* rounder shapes will exhibit lower specific resistance and will thus be more efficient. Another estimate of energy efficiency of a gait is the amount of travel in joint space that each module must move in order to move forward. This is measured by the difference between the two angles $\theta_a - \theta_s$. One approach is to use the shallow shape to accelerate quickly, then change the $\theta_a - \theta_s$ linearly with the speed. As it gets faster the shape becomes less oval and more circular. At the limit the shape will be that of a perfect circle which will roll using zero energy (assuming no energy is required to maintain its shape). It is worthwhile noting that, based on this measure, dynamic gaits with rounder shapes are also more efficient than kinematic gaits. Maintaining any velocity using a purely kinematic gait requires a fairly large traversal of joint space while, once some speed has been built up, dynamic gaits can be sustained using smaller effort in joint space.

5.2 Experimental results

Multiple rolling runs were conducted for different values of θ_a. The onboard controller on the robot determined which module was touching down at any instant and accordingly specified a desired shape for the robot. A range of shapes were tried ranging from rounder shapes ($\theta_a = 45^o$) to more elongated shapes ($\theta_a = 65^o$).

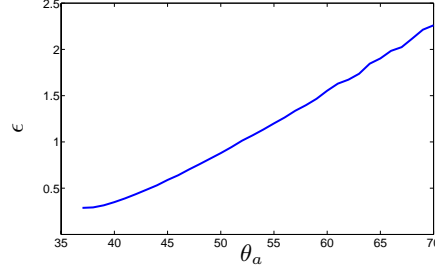**Fig. 6.** Simulation results: Specific resistance vs. θ_a
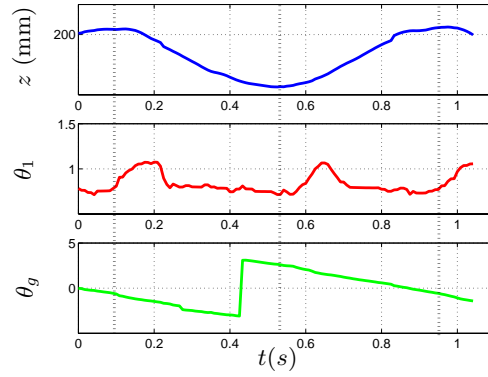

Fig. 7. Experimental results: Tracking θ_a for one module. Upper figure shows z position of tracked module over one complete revolution. Middle figure shows joint angle of tracked module in the world frame. Lower figure shows global rotation of tracked module (the discontinuity in the data is because of a jump from $-\pi$ to π).

Measurement of data was performed using a VICON motion capture system. The system is setup to provide accurate measurements of the position of the robot and one of the joint angles. This allowed comparison between the actual and desired trajectories of the joints on the robot and let us verify that the controller triggers the correct module on touchdown.

Figure 7 shows one such set of trajectories for one of the joints on the robot for the case where the controller tries to converge to $\theta_a = \pi/3$. Also plotted in the same figure is the z position of the module and the orientation of that module in the world frame. The crests in the z positions in Figure 7 represent touchdowns for the module diametrically opposite the tracked module while the troughs represent touchdowns for the tracked modules themselves. Figure 8 plots the average speed and compares the theoretical and experimental results. Below a certain magnitude of shape change, the robot has no terminal velocity since the energy input from shape change is insufficient to overcome the energy loss through impact. Thus, the
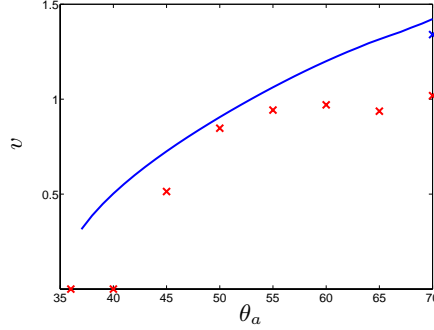
Fig. 8. Simulation (shown by a line) and experimental results (shown by markers): Final speed vs. θ_a

robot will undulate in place for gaits with parameters that restrict the amoun of shape change.

Although our experimental and simulation results are close, there is a discernible difference in the results. There may be several possible reasons for this difference in predicted and actual behavior. We have not taken into account friction in the modules and a motor model for the servos. Our model also assumes that the modules can be represented as rods (for determination of inertia parameters), however the actual modules have a complex shape that comes into contact with the ground.

6 Discussion

In this paper, we have analyzed the behavior of a dynamic rolling robot. We have shown through a combination of simulation and experiments that elongated shapes lead to higher terminal velocities while rounder shapes have lower specific resistance.The acceleration phase of the dynamic gait is similar to the motion of an inverted pendulum which has been shown in the context of walking to be very efficient requiring no work input to move the center of mass [6]. We believe higher rolling speeds should be more energy efficient (as modules on the top do not need to fight gravity due to the centrifugal force). Our conjecture about terminal velocities that more elongated desired shapes would have higher terminal velocities was confirmed by experiments. We also found that below a certain threshold, changing the shape will not produce rolling. Experimentally, we reported the fastest gait (1.4 m/s) for a battery powered modular robot. The use of sensors has improved the reliability of our gait. Proximity sensors may also allow us to build dynamic *conforming* gaits where the body of the robot conforms to the terrain it travels over.

Our future effort will also include the implementation of a speed controller, finding the optimal shape for maximum speed or maximum efficiency and attachment of more modules to enable steering. An advantage of our parameterization is that it is easily scalable and can be extended to loops with higher number of modules.

However, issues like low stiffness, higher weight and actuator limitations will hinder the performance of bigger loops.

Fig. 9. The motion of the robot is from right to left.

References

1. A. Castano, W. M. Shen, and P. Will. Conro: Towards deployable robots with inter-robot metamorphic capabilities. *Autonomous Robots Journal*, 8(3):309–324, July 2000.
2. G. S. Chirikjian. Kinematics of a metamorphic robotic system. In *Proceedings of the IEEE International Conference on Robotics and Automation*, pages 1452–1457, 1996.
3. Daniel Gomez-Ibanez, Ethan Stump, Ben Grocholsky, Vijay Kumar, and C. J. Taylor. The robotics bus: A local communications bus for robots. In *Proceedings of the Society of Photo-Optical Instrumentation Engineers*, 2004.
4. A. Kamimura, H. Kurokawa, E. Yoshida, S. Murata, and K. Tomita. Automatic locomotion design and experiments for a modular robotic system. *IEEE/ASME Transactions on Mechatronics*, 10(3):314–325, June 2005.
5. Akiya Kamimura, Satoshi Murata, Eiichi Yoshida, Haruhisa Kurokawa, Kohji Tomita, and Shigeru Kokaji. Self-reconfigurable modular robot - experiments on reconfiguration and locomotion. In *Proceedings of 2001 IEEE/RSJ International Conference on Intelligent Robots and Systems (IROS200)*, pages 606–612, Maui, Hawaii, October 2001.
6. A. D. Kuo, J. M. Donelan, and A. Ruina. Energetic consequences of walking like an inverted pendulum: Step-to-step transitions. *Exercise and Sport Science Review*, 33(2), 2005.
7. T. Matsuda and S. Murata. Stiffness distribution control - locomotion of closed link robot with mechanical softness. In *Proc. IEEE Int. Conf. Robotics and Automation*, pages 1491–1498, Orlando, Florida, May 2006.
8. Wei-Min Shen, Maks Krivokon, Harris Chiu, Jacob Everist, Michael Rubenstein, and Jagadesh Venkatesh. Multimode locomotion via superbot robots. In *Proc. IEEE Int. Conf. Robotics and Automation*, pages 2552–2557, Orlando, Florida, May 2006.
9. Y. Sugiyama, A. Shiotsu, M. Yamanaka, and S. Hirai. Circular/spherical robots for crawling and jumping. In *Proc. of the IEEE Int. Conf. on Robotics and Automation*, Barcelona, Spain, April 2005.
10. M. Yim. *Locomotion With A Unit-Modular Reconfigurable Robot*. PhD thesis, Stanford University, Palo Alto, CA, December 1994.